Structural and Biochemical Studies of Human Galanin: NMR Evidence for Nascent Helical Structures in Aqueous Solution†

Michael B. Morris,*,‡ Gregory B. Ralston,‡ Trevor J. Biden,§ Carol L. Browne,§ Glenn F. King,*,‡ and Tiina P. Iismaa§

Department of Biochemistry, University of Sydney, and Garvan Institute of Medical Research, St Vincent's Hospital, Sydney, Australia

Received November 30, 1994⊗

ABSTRACT: The 30-residue human neuropeptide, galanin, was shown to bind to rat insulinoma RINm5F cells and to inhibit glyceraldehyde-stimulated insulin secretion from these cells in a manner quantitatively similar to that of porcine galanin. Neither human nor porcine galanin stimulated Ca^{2+} mobilization in cultured human small cell lung carcinoma cells. Sedimentation equilibrium analysis of human galanin showed that it was strictly monomeric in aqueous solution, indicating that the peptide interacts with its receptor(s) as a monomer. The monomeric nature of the peptide makes it especially suitable for structural studies using NMR. Nuclear Overhauser enhancement spectroscopy experiments performed on galanin dissolved in aqueous solution (150 mM KCl, pH 4) at both 33 and 3 °C indicate that certain regions of the peptide are capable of adopting detectable levels of short-range structure in rapid equilibrium with random coil. At 33 °C, the short-range structures include a nascent helix spanning residues 3−11 which incorporates a hydrophobic core from residues 6−11. Residues 14−18 and 22−30 display sequential NH−NH and $C^{\beta}H$−NH connectivities, indicating that these regions of the peptide adopt nonrandom conformations by significantly populating the α-region of conformational space. However, no medium-range dipolar connectivities indicative of nascent helix or turn conformations were observed. At 3 °C, almost all residues significantly populate the α-region of conformational space, and the nascent helix between residues 3 and 11, with its hydrophobic core, is retained. As expected, circular dichroism (CD) was insensitive to the presence of short-range structure, and therefore the CD spectrum of human galanin in aqueous solution indicated a completely random coil peptide. However, changes in the CD spectrum resulting from the addition of 30% (v/v) of the helix-promoting organic solvent, trifluoroethanol, indicated that ~6 residues of the peptide were transformed to stable helix.

The neuropeptide galanin has a widespread distribution in the central and peripheral nervous system of mammals. In general, galanin decreases insulin secretion, blood pressure, pain, and sexual activity (Vrontakis et al., 1991; Ulman et al., 1992; Wiesenfeld-Hallin et al., 1992; Poggioli et al., 1992) and increases growth hormone secretion, heart rate, and appetite (Bauer et al., 1986; Kyrkouli et al., 1986; Ulman et al., 1992; Carey et al., 1993). It has species-specific contractile or relaxant effects on smooth muscle (Ekblad et al., 1985; Bauer et al., 1989; Rattan, 1991). Galanin has been reported to act as a mitogen in small cell lung carcinoma (SCLC)[1] cells (Sethi & Rozengurt, 1991) and is elevated in the hippocampus of Alzheimer's patients (Chan-Palay, 1988; Beal et al., 1991). Furthermore, the rat peptide inhibits the release of the neurotransmitter acetylcholine from neurons in the ventral hippocampus of the rat (Fisone et al., 1987) and appears to inhibit the acquisition of memory in this animal (Sundström et al., 1988; Ögren & Pramanik, 1991).

Galanin is expressed in a 123-residue prepro form which undergoes several posttranslational modifications. In the case of rat, porcine, and bovine galanin, the galanin peptide represents residues 33−62 of the prepro form (Rökaeus & Brownstein, 1986; Rökaeus & Carlquist, 1988). These peptides, together with those from sheep, dog, and chicken, are identical over the first 15 residues, and all are amidated at their C-termini (Tatemoto et al., 1983; Kaplan et al., 1988; Nörberg et al., 1991; Sillard et al., 1991; Boyle et al., 1994). The amidation results from the cleavage within the final glycine residue by the enzyme peptidylglycine α-amidating monooxygenase and generates a mature peptide of 29 residues (Eipper et al., 1992).

Human galanin (hGAL) is unique in that it contains 30 residues, since the prepro form contains a serine at position 62 which cannot be internally cleaved by the α-amidating monooxygenase (Evans & Shine, 1991). hGAL also contains a number of unique substitutions between residues 16 and 30 compared to galanins from other species, the most striking of which is the presence of a glycine residue at position 17 for the aspartate residue found in other mammalian galanins

† Supported by the National Health and Medical Research Council of Australia and in part by an Australian Research Council postdoctoral fellowship to M.B.M.

* Address correspondence to these authors (telephone, +61 2 3513902; Fax, +61 2 3514726; Email, michaelm@biochem.su.oz.au).
‡ University of Sydney.
§ Garvan Institute.

⊗ Abstract published in *Advance ACS Abstracts,* March 15, 1995.

[1] Abbreviations: 2D, two dimensional; BSA, bovine serum albumin; $C^{\alpha}H$, α-carbon proton; $C^{\beta}H$, β-carbon proton; $C^{\gamma}H$, γ-carbon proton; CD, circular dichroism; DQF-COSY, double-quantum-filtered correlated spectroscopy; TSP-d_4 3-(trimethylsilyl)[2,2,3,3-^2H]propionate; hGAL, human galanin; KRB, Krebs−Ringer buffer; NH, backbone amide proton; NOE, nuclear Overhauser effect; NOESY, nuclear Overhauser enhancement spectroscopy; pGAL, porcine galanin; ROESY, rotating-frame nuclear Overhauser enhancement spectroscopy; SCLC, small cell lung carcinoma; TOCSY, total correlation spectroscopy; Θ, mean residue ellipticity.

0006-2960/95/0434-4538$09.00/0

(Evans & Shine, 1991). These differences may explain the specific effects of human and other galanins observed in some *in vivo* and *in vitro* experiments (Miralles et al., 1990; Ulman et al., 1992).

The structure of *rat* galanin has been assessed using a variety of methods including CD, two-dimensional (2D) NMR, and molecular dynamics simulations (Wennerberg et al., 1990; Rigler et al., 1991; De Loof et al., 1992). Each of these studies indicated that the rat peptide is unstructured in aqueous solution and only adopts folded conformations in the presence of organic solvents such as trifluoroethanol (TFE).

In the present study, we use CD and 2D NMR spectroscopy to assess the structure of hGAL. The NMR results show that the human peptide adopts significant levels of short-range structure in aqueous solution which may provide recognition sites for the various galanin receptor subtypes as well as points of initiation of peptide folding following receptor binding.

MATERIALS AND METHODS

Synthesis of Human and Porcine Galanin. hGAL was synthesized using an Applied Biosystems 430A peptide synthesizer by standard *t*-Boc chemistry, with hydrogen fluoride cleavage using *p*-cresol as a scavenger (carried out by Auspep, Parkville, Victoria, Australia). The peptide was purified by high-performance liquid chromatography using a Deltapak C4 column and a linear gradient from 0 to 25% acetonitrile in 0.1% aqueous trifluoroacetic acid over 30 min. The preparations were lyophilized and stored desiccated at 4 °C. The molecular mass of synthesized hGAL was measured by electrospray mass spectrometry to be 3158, identical to the calculated value. Porcine galanin (pGAL) was purchased from Auspep.

Biological Activity of Synthetic Human Galanin. (i) Inhibition of Insulin Secretion. Galanin potently inhibits insulin secretion by direct action on pancreatic β-cells (Dunning et al., 1986; Su et al., 1987; Messell et al., 1990; Ahrén et al., 1991). This activity can be assayed *in vitro* by inhibiting glyceraldehyde-stimulated insulin secretion from rat insulinoma RINm5F cells (Ahrén et al., 1986; De Weille et al., 1988; Sharp et al., 1989).

RINm5F cells were grown to confluence in RPMI-1640 medium containing 24 mM $NaHCO_3$, 10% (v/v) fetal bovine serum, and 2 mM L-Gln in 5% CO_2−95% air at 37 °C. The confluent cells were detached from flasks using 0.025% (w/v) trypsin containing 0.02% (w/v) EDTA, pH 7.4, and were subsequently maintained in spinner flasks in Spinner medium [RPMI-1640 containing 1% (v/v) neonatal bovine serum] at an initial concentration of 4×10^6 cells/mL at 37 °C for 3 h. Cells were harvested by centrifugation at 800*g* for 10 min at room temperature. Cells were then rinsed twice in Krebs−Ringer buffer (KRB: 10 mM HEPES, pH 7.4, 136 mM NaCl, 4.7 mM KCl, 1.2 mM $MgSO_4$, 1.2 mM KH_2PO_4, 5 mM $NaHCO_3$, 2.8 mM glucose, and 1 mM $CaCl_2$) containing 0.5% (w/v) BSA and resuspended at a concentration of 10^6 cells/mL in fresh buffer. Aliquots of 10^6 cells were preincubated for 15 min at 37 °C and were then incubated for a further 15 min at 37 °C in the absence or presence of 10 mM glyceraldehyde, with or without the addition of hGAL or pGAL. Samples of the preincubation and incubation media were frozen for subsequent analysis. The concentration of insulin was determined by radioimmunoassay using ^{125}I-labeled human insulin as tracer and human insulin as standard.

(ii) Competitive Binding Studies. A particulate fraction comprising RINm5F cell membranes (Lagny-Pourmir et al., 1989) was resuspended in ice-cold buffer containing 50 mM Tris-HCl, pH 7.5, 100 mM NaCl, 5 mM EDTA, 100 μg/mL bacitracin, 100 μM phenylmethanesulfonyl fluoride, and 10 μg/mL leupeptin (Servin et al., 1987) and then stored at −70 °C. Protein concentration was determined by the method of Bradford (Bio-Rad Catalog No. 500-0006) using bovine γ-globulin as a standard. The binding of ^{125}I-pGAL to RINm5F cell membranes was carried out in a final volume of 250 μL of KRB containing 2% (w/v) BSA and 1 mg/mL bacitracin (Servin et al., 1987). Membranes (400 μg/mL) were incubated for 60 min at 15 °C in the presence of 0.2 nM ^{125}I-pGAL (2200 Ci/mmol; NEN-DuPont) and increasing concentrations of pGAL or hGAL (10^{-11}−10^{-6} M) and then were collected by centrifugation for 1 min through 1 mL of horse serum in a microcentrifuge. The supernatant containing free radioactivity was aspirated, and membrane-associated radioactivity was measured by counting pellets in a γ counter.

(iii) Calcium Mobilization in Human SCLC Cells (Woll & Rozengurt, 1989; Sethi & Rozengurt, 1991). NCI-H69 cells (ATCC HTB 119) were routinely grown in RPMI-1640 medium containing 24 mM $NaHCO_3$ and 10% (v/v) fetal bovine serum in 5% CO_2−95% air at 37 °C. Prior to use, cells were cultured for 3−5 days in serum-free medium [HITESA: RPMI-1640 containing 2 mM L-Gln, 10 nM hydrocortisone, 10 nM estradiol, 30 nM sodium selenite, 5 μg/mL insulin, 10 μg/mL transferrin, and 0.25% (w/v) BSA]. Aliquots of (4−5) $\times 10^6$ cells were washed, incubated for 2 h at 37 °C in 10 mL of fresh HITESA medium, and then incubated for 5 min in 1 mM fura-2 AM. The cells were harvested by centrifugation at 800*g* for 15 s, resuspended in 2 mL of KRB containing 200 μM sulfinpyrazone, and transferred to a quartz cuvette where they were stirred continuously. Concentrated stocks of hGAL, pGAL, and bradykinin were added at various times to give final concentrations of 10 nM, 100 nM, and 1 μM for each peptide. Fluorescence was recorded continuously in a Hitachi F-4010 fluorescence spectrophotometer with an excitation wavelength of 340 nm and an emission wavelength of 505 nm. The intracellular free calcium ion concentration, $[Ca^{2+}]_i$, was calculated using

$$[Ca^{2+}]_i = K_d(F - F_{min})/(F_{max} - F)$$

where F is the fluorescence at the unknown $[Ca^{2+}]_i$, F_{max} is the fluorescence after the trapped fura-2 AM is released by the addition of 0.04% (v/v) Triton X-100, and F_{min} is the fluorescence remaining after the Ca^{2+} in the solution is chelated with 4 mM EGTA. The value of K_d, the apparent dissociation constant for the complex of fura-2 AM and Ca^{2+}, was 225 nM.

Circular Dichroism. hGAL (0.1 mg/mL) in 5 mM potassium phosphate, pH 7.5, and 150 mM NaF ± 0−60% (v/v) TFE was loaded into a quartz cuvette (1-mm path length) and placed into an Aviv 62DS CD spectrometer (Department of Biochemistry, University of Melbourne)

equilibrated at 26 °C. Data were collected every 0.25 nm between 250 and 187 nm with a 1-s time constant and were smoothed using a sliding 15-point window.

Sedimentation Equilibrium. Three loading concentrations of hGAL (1.2, 0.6, and 0.3 g/L) in buffer containing 5 mM sodium phosphate, pH 7.5, and 150 mM KCl were loaded into a Yphantis 12-mm six-channel centerpiece to give solution column heights of 3 mm (Yphantis, 1964; Teller, 1973). The samples were centrifuged for 20 h at 20 °C at a speed of 30 000 rpm in an Optima XL-A analytical ultracentrifuge (Beckman). The concentration gradient of the peptide in each of the three channels was recorded at 280, 300, and 360 nm using the scanning absorbance optics in continuous radial mode. The step size was set at 10 μm, and the number of acquisitions for each step was set to 9. Scans were taken at 12, 16, and 20 h. Differences between the 16- and 20-h scans were within the precision of measurement, indicating that sedimentation equilibrium had been attained.

Absorbance values were converted to mass concentration using a calculated extinction coefficient (Gill & von Hippel, 1989) of 2.21. The concentration *versus* radial distance data in each of the three channels were fitted separately by nonlinear regression using a model which assumed a single, ideal, nonassociating molecule. This procedure returned a value for the molecular weight of the peptide ± the standard error. Data from the three different loading concentrations were also fitted simultaneously using the program NONLIN (Johnson et al., 1981).

^{1}H NMR. Galanin was resuspended to a concentration of ~1 mM in 95% H_2O/5% D_2O containing 5 mM potassium phosphate, pH 4.0, 150 mM KCl, and 1 mM NaN_3. Phase-sensitive double-quantum-filtered correlated spectroscopy (DQF-COSY), total correlated spectroscopy (TOCSY; Bax & Davis, 1985a). and rotating-frame nuclear Overhauser enhancement spectroscopy (ROESY; Bothner-By et al., 1984; Bax & Davis, 1985b) spectra were acquired at 33 °C using either a Bruker AMX 400-MHz wide-bore spectrometer or a Bruker AMX 600-MHz narrow-bore spectrometer. Nuclear Overhauser spectroscopy (NOESY; Kumar et al., 1980) spectra were acquired at 3 °C using the 600-MHz spectrometer. Time-proportional phase incrementation (Marion & Wüthrich, 1983) was used for quadrature detection in t_1. All spectra were collected over a chemical shift range of 11.5 ppm in both dimensions, centered on the HDO resonance. Suppression of the HDO resonance was effected during the relaxation delay (1.2−1.5 s) in all experiments as well as during the mixing periods of the ROESY and NOESY experiments. A 100-ms mixing time was used for the TOCSY experiments, 200 or 300 ms was used for the ROESY experiments, and 200 ms was used for the NOESY experiment. The spin-lock field strengths were 4.2 and 10 kHz for the ROESY and TOCSY experiments, respectively. A total of 450−512 t_1 points were collected with 80−144 scans for each t_1 increment and 2048 or 4096 complex points for each free induction decay.

Data were processed using a Gaussian window function in F_2, a shifted sine-bell window function in F_1, and zero filling or double zero filling in both dimensions prior to Fourier transformation. Chemical shifts were referenced to internal TSP-d_4 (0.00 ppm).

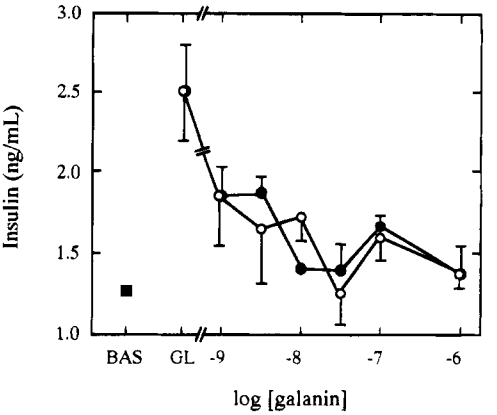

FIGURE 1: Inhibition of glyceraldehyde-stimulated insulin secretion from RINm5F cells. 10^6 cells were preincubated for 15 min at 37 °C and were then incubated for a further 15 min at 37 °C in the absence (■) or presence of 10 mM glyceraldehyde, with or without the addition of hGAL (●) or pGAL (○). Samples of incubation medium were frozen for subsequent analysis. Insulin concentration was determined by radioimmunoassay using ^{125}I-labeled human insulin as tracer and human insulin as standard. Error bars represent the standard deviations for triplicate measurements. For details see Materials and Methods. (BAS, basal level of insulin secretion; GL, glyceraldehyde in the absence of galanin.)

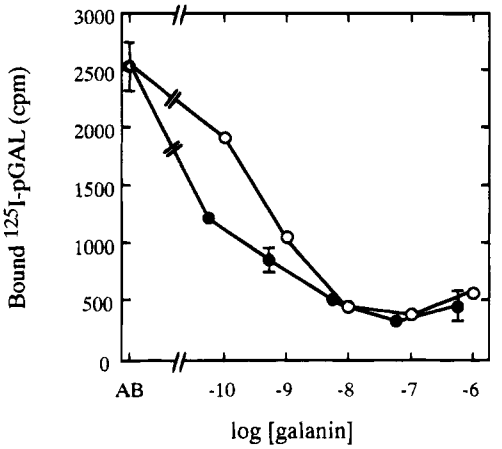

FIGURE 2: Displacement of ^{125}I-pGAL from RINm5F cell membranes by increasing concentrations of hGAL or pGAL. Membranes (0.4 g/L) were incubated for 60 min at 15 °C in the presence of 0.2 nM ^{125}I-pGAL with or without unlabeled hGAL (●) or pGAL (○) (10^{-11}−10^{-6} M). Error bars, most of which are smaller than the symbols, represent the standard deviations for triplicate measurements. For details see Materials and Methods. (AB, absence of unlabeled galanin.)

RESULTS

Biological Activity of Synthetic Human Galanin. Figure 1 shows that hGAL and pGAL are equally effective in inhibiting glyceraldehyde-stimulated insulin secretion from the rat insulin-secreting insulinoma cell line, RINm5F. The IC_{50} of ~1 nM is consistent with the results obtained by McKnight et al. (1992) for the inhibition of glucose-stimulated secretion from the related cell line RIN-5AH by hGAL and pGAL.

Figure 2 shows the displacement of ^{125}I-pGAL from the surface of the RINm5F cell membranes by unlabeled hGAL and pGAL. The IC_{50} for unlabeled pGAL is ~10^{-9} M while that for unlabeled hGAL is ~10^{-10} M, indicating that hGAL is at least as effective as pGAL in displacing ^{125}I-pGAL from the cell surface.

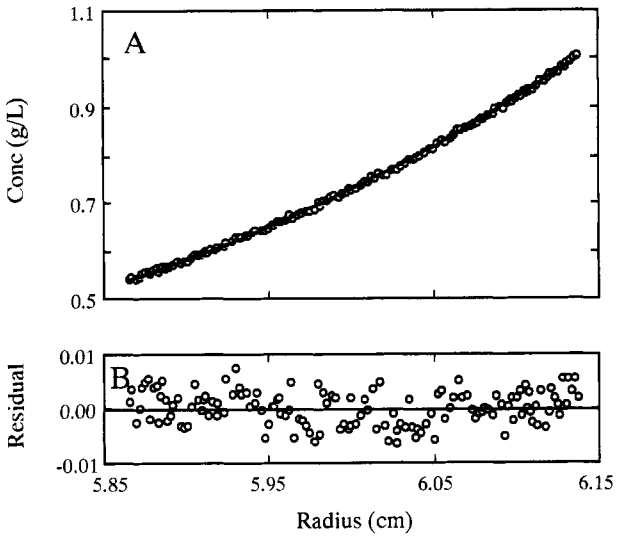

FIGURE 3: Sedimentation equilibrium analysis of hGAL. (A) shows a representative plot of mass concentration of peptide *versus* radial position for a single loading concentration of hGAL (0.3 g/L) centrifuged to sedimentation equilibrium in the analytical ultracentrifuge. Data were fitted using nonlinear regression with a model which assumed the presence of a single, ideal, nonassociating solute. The fit (solid line) returned a molecular weight of 3200 ± 120, equivalent to the calculated molecular weight of 3158 for monomeric hGAL. (B) shows that the distribution of the residuals of the fit is random.

Along with other peptides such as bradykinin and neurotensin, human galanin has been reported to stimulate calcium mobilization in the human SCLC cell line NCI-H69 (Woll & Rozengurt, 1989; Sethi & Rozengurt, 1991). However, contrary to published data, we did not observe an elevation of intracellular calcium levels in this cell line in response to the addition of either pGAL or hGAL (data not shown).

Analytical Ultracentrifugation. Figure 3A shows a plot of concentration *versus* radial position for a single loading concentration of hGAL centrifuged to sedimentation equilibrium. The concentration gradient has been fitted using nonlinear regression with a model that assumes the presence of a single, ideal, nonassociating solute. The random distribution of the residuals to the fit (Figure 3B) shows that the model is appropriate. The returned value of the molecular mass of the solute was 3200 ± 120, which is the same, within error, as the calculated molecular mass of 3158. The results from two other loading concentrations of hGAL, covering a range up to 1.3 mM, produced similar results. Simultaneous fitting of the data for all three loading concentrations returned a molecular mass of 3200 (2925–3384), where the numbers in parentheses represent the 95% confidence limits (Johnson et al., 1981). Collectively, these results show that hGAL behaves as a strictly ideal, monomeric peptide in solution and as such will not exhibit any concentration-dependent effects, even at the high concentrations of peptide used in NMR experiments (~1 mM).

Circular Dichroism Measurements. The CD spectrum of hGAL in the absence of organic solvent (Figure 4) is typical of random coil peptides with a minimum mean residue ellipticity (Θ) occurring at ~200 nm and with little variation in the value of Θ above 215 nm (Perczel et al., 1992). With increasing concentrations of TFE up to 30% (v/v), however, the spectral minimum shifted to 206 nm and a shoulder appeared at 222 nm, indicating the presence of stable helical conformations. In the presence of 30–60% TFE, Θ_{222} is ≈

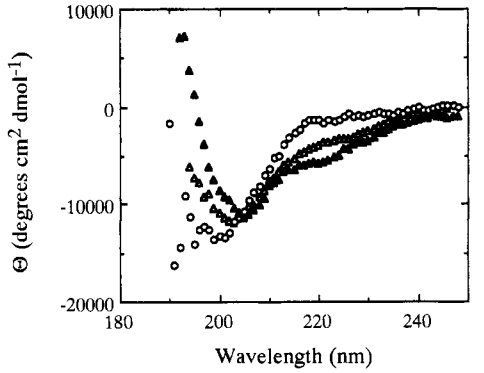

FIGURE 4: CD spectra of hGAL in aqueous solution (○) and in the presence of 20% (△) and 50% (▲) TFE. No detectable changes in the CD spectra occurred with concentrations of TFE of 30% or higher. For clarity, data are shown at ~1-nm intervals. Θ indicates the mean residue ellipticity.

−6000 deg cm² dmol⁻¹, indicating an average helical content of ~20%, which corresponds to ~6 residues or two turns of helix (Chen et al., 1974).

The CD spectra also show an isodichroic point at 205 nm, indicating a two-state transition between apparently random coil conformations and stable helix (Dyson et al., 1988a).

NMR Experiments. TFE can induce helix formation in those portions of peptides which significantly occupy the α-region of conformational space (Dyson et al., 1988a, 1992). In particular, the presence of the short-range structure known as nascent helix is a strong indicator of the potential for folding into stable helix (Dyson et al., 1988a). All of these short-range structures, including nascent helix, are thermodynamically unstable and in rapid dynamic equilibrium with random coil conformations (Dyson et al., 1988a,b). Those short-range structures which have the potential to form stable helix cannot be distinguished from random coil conformations using CD. However, their presence can be detected using 2D NMR (see below).

The combination of DQF-COSY, TOCSY, and ROESY spectra of hGAL recorded at 33 °C allowed unambiguous sequence-specific assignment of all spin systems (see the table in the supplementary material). The use of NOESY proved unsuitable at this temperature. Very few cross-peaks were observed, presumably because the molecular correlation time resulted in a nuclear Overhauser enhancement of approximately zero.

Figure 5A shows the chemical shift differences from random coil positions for all observable $C^{\alpha}H$. The plot indicates that both the N- and C-terminal halves of the peptide contain regions whose $C^{\alpha}H$ show significant departures from random coil positions. These data indicate that portions of the N- and C-terminal halves of the peptide adopt detectable levels of structured conformations which are in rapid equilibrium with the ensemble of random coil conformations.

Figure 6 shows representative areas of a ROESY spectrum obtained at 33 °C, while Figure 5B summarizes the interresidue NOE (through-space) connectivities observed for hGAL at this temperature. The strong sequential $d_{\alpha N}(i,i+1)$ connectivities across the whole peptide are indicative of extended conformations. These extended conformations are heavily populated by small peptides undergoing predominantly random coil motions (Dyson et al., 1988a).

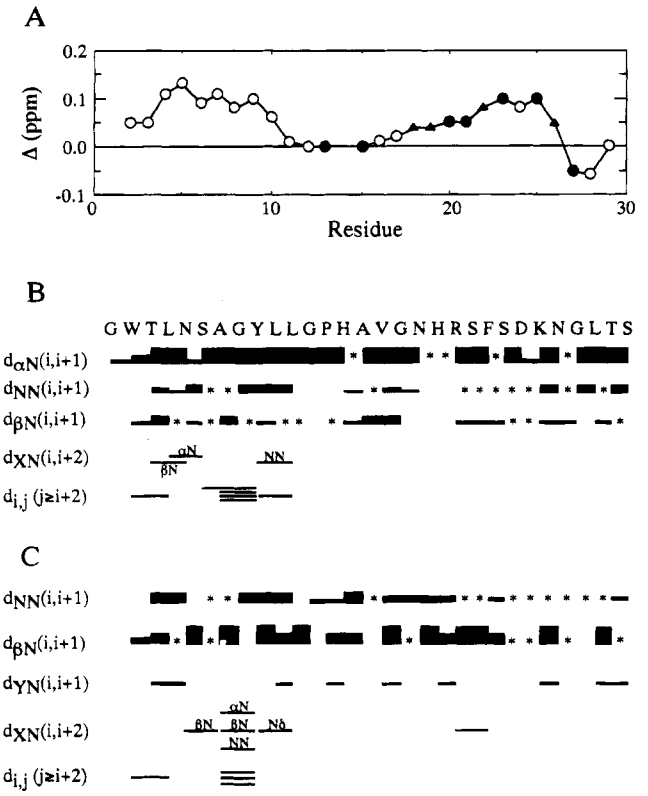

FIGURE 5: (A) Chemical shift differences from random coil positions for C^{α} protons of hGAL at 33 °C. Positive values represent shifts that are upfield from the random coil values (Wüthrich, 1986). Open circles represent the average value for the residue and its nearest neighbor on either side. Closed circles represent the average value for the residue and its nearest neighbor on one side, where the resonance on the other side could not be observed due to overlap with the HDO resonance. Results obtained at 3 °C were almost identical to those at 33 °C. The triangles represent values obtained at 3 °C which could not be observed at 33 °C. (B) and (C) show a summary of the interresidue NOE cross-peaks for hGAL observed at 33 and 3 °C, respectively. The thickness of the bars is indicative of the intensity of the cross-peaks. Designations of the $d_{XN}(i,i+2)$ connectivities are shown above the bars. For the $d_{YN}(i,i+1)$ connectivities, Y ≡ $C^{\gamma}H$, $C^{\delta}H$, ..., while $d_{i,j}$ represents connectivities between side-chain protons. The asterisks represent $d_{NN}(i,i+1)$ and $d_{\beta N}(i,i+1)$ cross-peaks that may be present but which could not be observed due to resonance overlap.

There are three regions of sequential $d_{NN}(i,i+1)$ connectivities from residues 3−11, 14−18, and 25−30 (Figure 5B and 6A). These connectivities are not observed in random coil peptides, except that an NOE cross-peak between the amide protons of the final two residues is seen frequently in peptides which are otherwise fully random coil (Dyson et al., 1988a). The $d_{\beta N}(i,i+1)$ connectivities generally coincide with the $d_{NN}(i,i+1)$ connectivities as well as with the significant departures of $C^{\alpha}H$ resonances from random coil positions (see Figure 5A,B). These connectivities are also not observed in fully random peptides (Dyson et al., 1988a). Together, these data support the interpretation that defined regions of hGAL, residues 3−11, 14−18, and 22−30, are capable of adopting detectable levels of nonrandom conformations by significantly populating the α-region of conformational space (Dyson et al., 1988a).

Also listed in Figure 5B are the three medium-range NOEs to backbone amide protons observed in the N-terminal half of the peptide. These medium-range NOEs indicate the presence of nascent helix in the region between residues 3

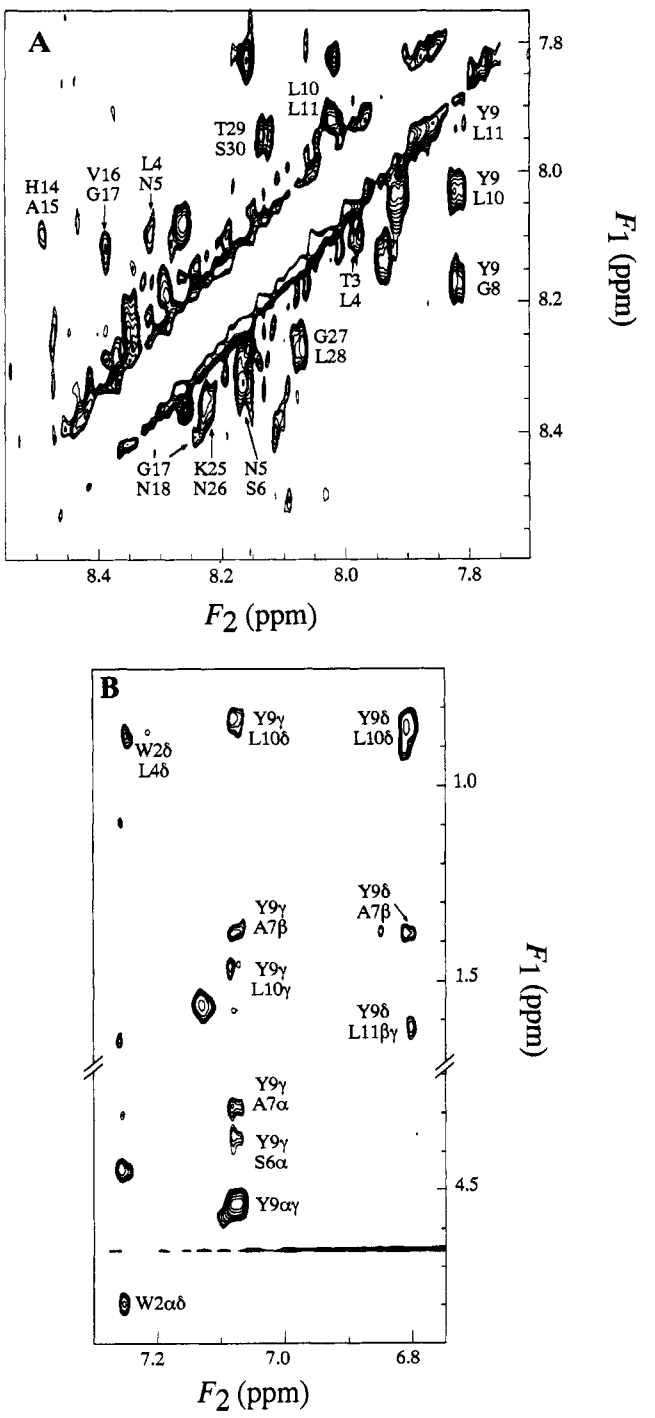

FIGURE 6: Portions of a 600-MHz NMR ROESY spectrum of hGAL at 33 °C showing (A) NH−NH connectivities and (B) side-chain−side-chain NOE cross-peaks between Tyr9 and residues 6, 7, 10, and 11 and between Trp2 and Leu4. In (A), the NH−NH cross-peak between Tyr9 and Leu11 can be seen more clearly at contour levels closer to the baseline.

and 11. It is this part of the peptide that is most likely to adopt stable helical structures in the presence of TFE as observed by CD (Figure 4). The absence of similar medium-range NOEs from residues 14−18 and 22−30 at 33 °C indicates that these regions do not form nascent helix, although they are still capable of adopting nonrandom conformations.

The dipolar connectivities observed at 3 °C in the NOESY spectrum are summarized in Figure 5C. There is an increase in the number of sequential NH−NH and $C^{\beta}H$−NH con-

nectivities observed at this temperature compared to those at 33 °C (Figure 5B,C). In addition, there are several sequential CH−NH connectivities involving protons beyond the $C^{\beta}H$ of the individual side chains (Figure 5C). The nascent helix from residues 3−11, as measured by the presence of $d_{XN}(i,i+2)$ connectivities, is retained at 3 °C (Figure 5C).

Hydrophobic Core. Several NOEs were observed between side-chain protons in the hydrophobic region Ser6-Ala7-Gly8-Tyr9-Leu10-Leu11 at both 33 and 3 °C. In particular, the Tyr9 side-chain protons show through-space connectivities with protons from all other side chains in this sequence except Gly8 (Figure 6B), indicating a partially stable hydrophobic core centered around Tyr9. In addition, the Gly8 $C^{\alpha}H$ are nonequivalent, indicating that these backbone protons spend a significant proportion of their time in an asymmetric environment. In contrast, the $C^{\alpha}H$ for the two other nonterminal glycine residues are equivalent.

An NOE was also observed between the 2H proton of the Trp2 side chain and the $C^{\delta}H$ of Leu4, indicating that both the N- and C-terminal ends of the nascent helix between residues 3 and 11 are bounded by residues whose side chains interact hydrophobically.

Cis−Trans Isomerism. hGAL contains a single proline at position 13. Spectra from dipolar coupling experiments show a strong connectivity between the Gly12 C^{α} protons and the δ protons of the proline, indicating that the proline is predominantly in the *trans* form (Wüthrich et al., 1984; Dyson et al., 1988b). It is also clear from scalar and dipolar coupling spectra that additional weak cross-peaks are also visible for residues from Leu10 to Val16. We attribute this second set of cross-peaks to the *cis* conformer of proline. The cross-peaks are shifted either upfield or downfield with respect to those cross-peaks of the *trans* isomer (see the table in the supplementary material). In ROESY spectra, an NOE occurs between one of the secondary peaks assigned to Gly12 $C^{\alpha}H$ and a secondary peak assigned to $C^{\alpha}H$ of Pro13. This is consistent with the presence of a *cis* proline (Wüthrich et al., 1984; Dyson et al., 1988b). The two sets of distinct peaks indicate a slow exchange (on the NMR time scale) between the *cis* and *trans* forms. The relative volumes of the Pro13 cross-peaks in TOCSY spectra arising from both the *cis* and *trans* isomers indicate that ~90% of the peptide is in the *trans* form at any one time.

DISCUSSION

Synthetic hGAL was equipotent with pGAL in inhibiting insulin secretion from rat insulinoma RINm5F cells and in displacing radiolabeled pGAL from the surface of these cells (Figures 1 and 2). Furthermore, the IC_{50} values for the inhibition of insulin secretion and for the displacement of radiolabeled galanin from the cell membranes were consistent with published values (Schmidt et al., 1991; McKnight et al., 1992). Together, these data indicate that the synthetic human and porcine peptides had native biological and physical properties. In spite of this, neither peptide was able to mediate mobilization of calcium in SCLC cells, although, as expected, mobilization was readily observed using bradykinin. In contrast, recent published results (Woll & Rozengurt, 1989) report mobilization of calcium by galanin in the same system. At present we do not understand the reasons for these differences.

Sedimentation equilibrium experiments show that galanin remains strictly monomeric even at concentrations above 1 mM. This indicates that galanin *in vivo* interacts with its receptors as a monomer, an important result in terms of the pharmacology of its action. In addition, the strictly monomeric nature of the peptide greatly simplifies interpretation of the NMR data. In particular, NOE cross-peaks in ROESY and NOESY spectra of a monomer will arise only from intramolecular connectivities whereas, in a polymerizing system, it will not be clear whether the cross-peaks result from intra- or interpeptide connectivities. Even small amounts of polymer can seriously affect the interpretation of the spectra obtained from dipolar coupling experiments, since the NOE cross-peaks will build up more rapidly in larger complexes (Waltho et al., 1993).

It is clear that in aqueous solution hGAL does not adopt highly folded conformations. Instead, selected regions of the peptide adopt short-range structures which are in rapid equilibrium with random coil conformations.

The most structured region lies from Thr3 to Leu11 where the presence of relatively strong, sequential NH−NH and $C^{\beta}H$−NH connectivities indicate that the α-region of conformational space is significantly populated (Figures 5 and 6). In addition, the presence of medium-range connectivities to backbone amide protons in this part of the peptide indicates the presence of nascent helix (Figure 5B,C). No other connectivities indicative of a stable helix, such as $d_{\beta N}(i,i+3)$ or $d_{\alpha N}(i,i+3)$, were observed. However, a stable helix could be induced in the peptide by the addition of the helix-promoting solvent, TFE. TFE has been observed to induce helix formation only in those parts of a peptide which significantly populate the α-region of conformational space. Regions of a peptide that are completely random coil (or that populate turn conformations), as observed by NMR, do not adopt a stable helix in the presence of TFE (Dyson et al., 1988a, 1992; Shin et al., 1993).

The estimated helix content of galanin in the presence of 30−60% TFE is 6−7 residues (or ~2 turns of helix), which is similar to the number of residues which appear to adopt nascent helix in the N-terminal half of the peptide. It should be noted, however, that the ability of CD to detect a stable helix will be greatly compromised where even small distortions of the backbone carbonyl chromophores from regular helical geometries occur (Manning et al., 1988) or where the length of the helix is less than ~2 turns (Goodman et al., 1969; Madison & Schellman, 1972). Thus, estimates of helix using CD are likely to represent lower bounds.

The nascent helix includes a hydrophobic core centered on Tyr9 (Figure 6B). The relative insensitivity of the nascent helix to changes in temperature may reflect the importance of hydrophobic interactions on the stability of this region. A similar situation occurs with the 19-residue C-helix peptide of myohemerythrin whose nascent helix is centered on a hydrophobic core (Dyson et al., 1988a).

The combination of nascent helix with a hydrophobic core indicates the potential for this region to act as a point of initiation of folding when, for example, the peptide binds to its receptor (Lim, 1980; Baldwin, 1986; Dyson et al., 1988a; Zhou et al., 1992). Indeed, the short-range structure of this region may act as a point of recognition for the receptor. Analogous situations have been observed with peptides in aqueous solution whose sequences are identical to those in a folded protein. For example, the C-helix of myohem-

erythrin, which is α-helical along its entire length in the native protein, does not form a stable helix when isolated in aqueous solution (Dyson et al., 1988a). However, the C-terminal half of the isolated peptide adopts nascent helical structure in aqueous solution which can be stabilized in the presence of TFE (Dyson et al., 1988a). This half of the C-helix in the intact protein may act as a point of initiation of protein folding very early in the folding process (Dyson et al., 1988a). Furthermore, the C-terminal portion of the C-helix peptide is immunogenic; antibodies raised to this peptide cross-react with the stable α-helix in the native protein. These data indicate that, while the isolated C-helix has only short-range structure in solution, it must adopt a folded conformation close to that found in the native protein when the peptide is bound to carrier protein or when it is bound to the B-cell receptor (Dyson et al., 1988c).

By analogy, the N-terminal region of galanin, which is capable of adopting short-range structural motifs in aqueous solution, may provide the platform for receptor recognition and a point of initiation of folding to more stable conformations upon binding to receptor. Such a hypothesis is consistent with the completely conserved nature of the N-terminal region of the peptide across mammalian and avian species including rat, pig, cow, dog, human, sheep, and chicken (Evans & Shine, 1991; Nörberg et al., 1991; Sillard et al., 1991; Boyle et al., 1994). In addition, the N-terminal half of galanin is frequently able to bind a variety of receptor subtypes where it acts as an agonist (Amiranoff et al., 1989; Fisone et al., 1989; Crawley et al., 1990; Gregersen et al., 1991; Xu et al., 1990). Furthermore, Trp9, which lies at the center of the hydrophobic core, has been demonstrated to be of particular importance in high-affinity binding of galanin to receptors in the rat hippocampus (Fisone et al., 1991).

The role of Pro13 in the peptide is at present ambiguous. Pro13 may act as a helix stop signal or form the second residue in a β-turn. Evidence for a β-turn is scant under the conditions of the NMR experiments that we have used. The presence of both *cis* and *trans* conformations of the Pro13 is expected. However, even though the *trans* isomer predominates in solution, it is possible that the *cis* isomer is stabilized upon binding to the receptor (Dyson et al., 1992). Furthermore, the *cis* isomer is likely to influence strongly the local structure of the peptide. It is clear that for hGAL in aqueous solution the chemical shifts of residues from Leu10 to Val16 are significantly changed in the *cis* isomer relative to the *trans* isomer (see table in the supplementary material). The NOEs associated with the *cis* isomer, however, are too weak to ascertain whether any short-range structure such as a β-turn is present (Dyson et al., 1988b).

The C-terminal half of hGAL also significantly accesses the α-region of conformational space (Figure 5B). However, unlike the N-terminal region between residues 3 and 11, only one medium-range NOE indicative of nascent helix is observed at 3 °C and there are no side-chain interactions indicative of a hydrophobic core. Nevertheless, portions of peptides which access the α-region of conformational space do have the potential to fold into secondary structure following stabilization through, for example, the addition of TFE or contact with a receptor (Dyson et al., 1988a, 1992; Shin et al., 1993; Waltho et al., 1993). Thus, such regions may fold after appropriate additional interactions.

The apparently less stable nature of the C-terminal half of hGAL compared to the N-terminal half correlates with a generally reduced ability of C-terminal peptides to bind to galanin receptors and elicit agonist or antagonist effects (Fox et al., 1988; Murakami et al., 1989; Kuwahara et al., 1990; Xu et al., 1990; Ulman et al., 1993). However, the cases where effects are observed (Ekblad et al., 1985; Fox et al., 1988; Fisone et al., 1989; Rossowski et al., 1990) may reflect the ability of these shortened peptides to be recognized by, and to adopt secondary structure once bound to, particular subsets of galanin receptors.

In summary, the conserved N-terminal half of hGAL, between residues 3 and 11, is capable of adopting nascent helix in aqueous solution. Presumably, it is this region which adopts a stable helix upon the addition of TFE. Pro13 may act as a helix-stop signal. The C-terminal end of the peptide (residues 22−30) can access the α-region of conformational space. This region may be recognized by, and bind sufficiently strongly to, some receptor subtypes and adopt stable secondary structure upon binding.

Our results contrast with those obtained by Wennerberg et al. (1990), who did not observe short-range structure in rat galanin in aqueous solution at 30 °C using NOESY. However, a stable helix was formed in TFE, indicating that the rat peptide probably does form short-range structure under these conditions. We found NOESY to be unsuitable for structural analysis of hGAL at 33 °C since the nuclear Overhauser enhancement was close to, or at, the NOE null for almost all dipolar connectivities. Presumably, NOESY is equally unsuitable for the rat peptide.

ACKNOWLEDGMENT

We thank Dr. Bill Bubb for expert maintenance of the Bruker AMX 400 and AMX 600 spectrometers and Prof. Bill Sawyer for access to the Aviv 62DS CD spectrometer. Adam Inglis and Albert Tseng are thanked for their expert assistance in the synthesis of human galanin, and Dr. Barbara Kofler is thanked for helpful discussions.

SUPPLEMENTARY MATERIAL AVAILABLE

A table listing the resonance assignments of hGAL (1 page). Ordering information is given on any current masthead page.

REFERENCES

Ahrén, B., Taborsky, G. J., & Porte, D. (1986) *Diabetologia 29*, 827−836.

Ahrén, B., Ar'Rajab, A., Böttcher, G., Sundler, F., & Dunning, B. E. (1991) *Cell Tissue Res. 264*, 263−267.

Amiranoff, B., Lorinet, A. M., Yanaihara, N., & Laburthe, M. (1989) *Eur. J. Pharmacol. 163*, 205−207.

Baldwin, R. L. (1986) *Trends Biochem. Sci. 11*, 6−9.

Bauer, F. E., Venetikou, M., Burrin, J. M., Ginsberg, L., MacKay, D. J., & Bloom, S. R. (1986) *Lancet 2*, 192−194.

Bauer, F. E., Zintel, A., Kenny, M. J., Calder, D., Ghatel, M. A., & Bloom, S. R. (1989) *Gastroenterology 97*, 260−264.

Bax, A., & Davis, D. G. (1985a) *J. Magn. Reson. 65*, 355−360.

Bax, A., & Davis, D. G. (1985b) *J. Magn. Reson. 63*, 207−213.

Beal, M. F., MacGarvey, U., & Swartz, K. J. (1991) *Ann. Neurol. 28*, 157−161.

Bothner-By, A. A., Stephens, R. L., Lee, J. M., Warren, C. D., & Jeanloz, R. W. (1984) *J. Am. Chem. Soc. 106*, 811−813.

Boyle, M. R., Verchere, C. B., McKnight, G., Mathews, S., Walker, K., & Taborsky, G. J. (1994) *Regul. Pept. 50*, 1−11.

Carey, D. G., Iismaa, T. P., Ho, K. K., Rajkovic, I. A., Kelly, J., Kraegen, E. W., Ferguson, J., Inglis, A. S., Shine, J., & Chisholm, D. J. (1993) *J. Clin. Endocrinol. Metab. 77*, 90−93.
Chan-Palay, V. (1988) *J. Comp. Neurol. 273*, 543−557.
Chen, Y. H., Yang, J. T., & Chau, K. H. (1974) *Biochemistry 13*, 3350−3359.
Crawley, J. N., Austin, M. C., Fiske, S. M., Martin, B., Consolo, S., Berthold, M., Langel, Ü., Fisone, G., & Bartfai, T. (1990) *J. Neurosci. 10*, 3695−3700.
De Loof, H., Nilsson, L., & Rigler, R. (1992) *J. Am. Chem. Soc. 114*, 4028−4035.
De Weille, J., Schmid-Antomarchi, H., Fosset, M., & Lazdunski, M. (1988) *Proc. Natl. Acad. Sci. U.S.A. 85*, 1312−1316.
Dunning, B. E., Ahrén, B., Veith, R. C., Böttcher, G., Sundler, F., & Taborsky, G. J. (1986) *Am. J. Physiol. 251*, E127−E133.
Dyson, H. J., Rance, M., Houghten, R. A., Wright, P. E., & Lerner, R. A. (1988a) *J. Mol. Biol. 201*, 201−217.
Dyson, H. J., Rance, M., Houghten, R. A., Lerner, R. A., & Wright, P. E. (1988b) *J. Mol. Biol. 201*, 161−200.
Dyson, H. J., Lerner, R. A., & Wright, P. E. (1988c) *Annu. Rev. Biophys. Biophys. Chem. 17*, 305−324.
Dyson, H. J., Sayre, J. R., Merutka, G., Shin, H. C., Lerner, R. A., & Wright, P. E. (1992) *J. Mol. Biol. 226*, 795−817.
Eipper, B. A., Stoffers, D. A., & Mains, R. E. (1992) *Annu. Rev. Neurosci. 15*, 57−85.
Ekblad, E., Håkanson, R., Sindler, F. & Wahlestedt, C. (1985) *Br. J. Pharmacol. 213*, 87−90.
Evans, H. F., & Shine, J. (1991) *Endocrinology 129*, 1682−1684.
Fisone, G., Wu, G. F., Consolo, S., Nordström, Ö., Brynne, N., Bartfai, T., Melander, T., & Hökfelt, T. (1987) *Proc. Natl. Acad. Sci. U.S.A. 84*, 7339−7343.
Fisone, G., Langel, Ü., Carlquist, M., Bergman, T., Consolo, S., Hökfelt, T., Unden, A., Andell, S., & Bartfai, T. (1989) *Eur. J. Biochem. 181*, 269−276.
Fisone, G., Langel, Ü., Land, T., Berthold, M., Bertorelli, R., Girotti, P., Consolo, S., Crawley, J. N., Hökfelt, T., & Bartfai, T. (1991) in *Galanin. A New Multifunctional Peptide in the Neuroendocrine System* (Hökfelt, T., Bartfai, T., Jacobowitz, D., & Ottosson, D., Eds.) pp 213−220, Macmillan, London.
Fox, J. E. T., Brooks, B., McDonald, T. J., Barnett, W., Kostolanska, F., Yanaihara, C., Yanaihara, N., & Rökaeus, Å. (1988) *Peptides 9*, 1183−1189.
Gill, S. C., & von Hippel, P. H. (1989) *Anal. Biochem. 182*, 319−326.
Goodman, M., Verdini, A. S., Toniolo, C., Phillips, W. D., & Bovey, F. A. (1969) *Proc. Natl. Acad. Sci. U.S.A. 64*, 444−450.
Gregersen, S., Hermanse, K., Yanaihara, N., & Ahrén, B. (1991) *Pancreas 6*, 216−220.
Johnson, M. L., Correia, J. J., Yphantis, D. A., & Halvorson, H. R. (1981) *Biophys. J. 36*, 575−588.
Kaplan, L. M., Spindel, E. R., Isselbacher, K. J., & Chin, W. W. (1988) *Proc. Natl. Acad. Sci. U.S.A. 85*, 1065−1069.
Kumar, A., Ernst, R. R., & Wüthrich, K. (1980) *Biochem. Biophys. Res. Commun. 95*, 1−6.
Kuwahara, A., Ozaki, T., & Yanaihara, N. (1990) *Regul. Pept. 29*, 23−29.
Kyrkouli, S. E., Stanley, B. G., & Leibowitz, S. F. (1986) *Eur. J. Pharmacol. 122*, 159−160.
Lagny-Pourmir, I., Amiranoff, B., Lorinet, A. M., Tatemoto, K., & Laburthe, M. (1989) *Endocrinology 124*, 2635−2641.
Lim, V. (1980) in *Protein Folding* (Jaenicke, R., Ed.) pp 149−166, Elsevier, Amsterdam.
Madison, V., & Schellman, J. (1972) *Biopolymers 11*, 1041−1076.
Manning, M. C., Illangasekare, M., & Woody, R. W. (1988) *Biophys. Chem. 31*, 77−86.
Marion, D., & Wüthrich, K. (1983) *Biochem. Biophys. Res. Commun. 113*, 967−974.
McKnight, G. L., Karlsen, A. E., Kowalyk, S., Mathewes, S. L., Sheppard, P. O., O'Hara, P. J., & Taborsky, G. J. (1992) *Diabetes 41*, 82−87.
Messell, T., Harling, H., Böttcher, F., Johnsen, A. H., & Holst, J. J. (1990) *Regul. Pept. 28*, 161−176.
Miralles, P., Peiro, E., Degano, P., Silvestre, R. A., & Marco, J. (1990) *Diabetes 39*, 996−1001.
Murakami, Y., Kato, Y., Shimatsu, A., Koshiyama, H., Hattori, N., Yanaihara, N., & Imura, H. (1989) *Endocrinology 124*, 1224−1229.
Nörberg, Å., Sillard, R., Carlquist, M., Jörnvall, H., & Mutt, V. (1991) *FEBS Lett. 288*, 151−153.
Ögren, S. O., & Pramanik, A. (1991) in *Cholinergic Basis for Alzheimer Therapy* (Becker, R. E., & Giacobini, E., Eds.) pp 193−199, Birkhäuser, Boston.
Perczel, A., Park, K., & Fasman, G. D. (1992) *Proteins 13*, 57−69.
Poggioli, R., Rasori, E., & Bertolini, A. (1992) *Eur. J. Pharmacol. 213*, 87−90.
Rattan, S. (1991) *Gastroenterology 100*, 1762−1768.
Rigler, R., Wennerberg, A., Cooke, R. M., Elofsson, A., Nilsson, L., Vogel, H., Holley, L. H., Carlquist, M., Langel, Ü., Bartfai, T., & Campbell, I. D. (1991) in *Galanin. A New Multifunctional Peptide in the Neuro-Endocrine System* (Hökfelt, T., Bartfai, T., Jacobowitz, D., & Ottoson, D., Eds.) pp 17−25, Macmillan, London.
Rökaeus, Å., & Brownstein, M. J. (1986) *Proc. Natl. Acad. Sci. U.S.A. 83*, 6287−6291.
Rökaeus, Å., & Carlquist, M. (1988) *FEBS Lett. 234*, 400−406.
Rossowski, W. J., Rossowski, S., Zacharia, S., Ertan, A., & Coy, D. H. (1990) *Peptides 11*, 333−338.
Schmidt, W. E., Kratzin, H., Eckart, K., Drevs, D., Mundowski, G., Clemens, A., Katsoulis, S., Schäfer, H., Gallwitz, B., & Creutzfeldt, W. (1991) *Proc. Natl. Acad. Sci. U.S.A. 88*, 11435−11439.
Servin, A. L., Amiranoff, B., Rouyer-Fessard, C., Tatemoto, K., & Laburthe, M. (1987) *Biochem. Biophys. Res. Commun. 144*, 298−306.
Sethi, T., & Rozengurt, E. (1991) *Cancer Res. 51*, 1674−1679.
Sharp, G. W. G., Le Marchand-Brustel, Y., Yada, T., Russo, L. L., Bliss, C. R., Cormont, M., Monge, L., & Van Obberghen, E. (1989) *J. Biol. Chem. 264*, 7302−7309.
Shin, H. C., Merutka, G. Waltho, J. P., Wright, P. E., & Dyson, H. J. (1993) *Biochemistry 32*, 6348−6355.
Sillard, R., Langel, Ü., & Jörnvall, H. (1991) *Peptides 12*, 855−859.
Su, H. C., Bishop, A. E., Power, R. F., Hamada, Y., & Polak, J. M. (1987) *J. Neurosci. 7*, 2674−2687.
Sundström, E., Archer, T., Melander, T., & Hökfelt, T. (1988) *Neurosci. Lett. 88*, 331−335.
Tatemoto, K., Rökaeus, Å., Jörnvall, H., McDonald, T. J., & Mutt, V. (1983) *FEBS Lett. 164*, 124−128.
Teller, D. C. (1973) *Methods Enzymol. 27*, 346−441.
Ulman, L. G., Evans, H. F., Iismaa, T. P., Potter, E. K., McCloskey, D. I., & Shine, J. (1992) *Neurosci. Lett. 136*, 105−108.
Ulman, L. G., Potter, E. K., & McCloskey, D. I. (1993) *Regul. Pept. 44*, 85−92.
Vrontakis, M. E., Torsello, A., & Friesen, H. G. (1991) *J. Endocrinol. Invest. 14*, 785−794.
Waltho, J. P., Feher, V. A., Merutka, G., Dyson, H. J., & Wright, P. E. (1993) *Biochemistry 32*, 6337−6347.
Wennerberg, A. B. A., Cooke, R. M., Carlquist, M., Rigler, R., & Campbell, I. D. (1990) *Biochem. Biophys. Res. Commun. 166*, 1102−1109.
Wiesenfeld-Hallin, Z., Xu, X.-J., Langel, Ü., Bedecs, K., Hökfelt, T., & Bartfai, T. (1992) *Proc. Natl. Acad. Sci. U.S.A. 89*, 3334−3337.
Woll, P. J., & Rozengurt, E. (1989) *Biochem. Biophys. Res. Commun. 164*, 66−73.
Wüthrich, K. (1986) in *NMR of Proteins and Nucleic Acids*, Wiley, New York.
Wüthrich, K., Billeter, M., & Braun, W. (1984) *J. Mol. Biol. 180*, 715−740.
Xu, X. J., Wiesenfeld-Hallin, Z., Fisone, G., Bartfai, T., & Hökfelt, T. (1990) *Eur. J. Pharmacol. 128*, 137−141.
Yphantis, D. A. (1964) *Biochemistry 3*, 297−317.
Zhou, N. E., Zhu, B. Y., Sykes, B. D., & Hodges, R. S. (1992) *J. Am. Chem. Soc. 114*, 4320−4326.

BI942760Q